

## Atomic mobility in nanostructured liquid Ga–In alloy

This article has been downloaded from IOPscience. Please scroll down to see the full text article.

2010 J. Phys.: Condens. Matter 22 195108

(<http://iopscience.iop.org/0953-8984/22/19/195108>)

View [the table of contents for this issue](#), or go to the [journal homepage](#) for more

Download details:

IP Address: 129.252.86.83

The article was downloaded on 30/05/2010 at 08:06

Please note that [terms and conditions apply](#).

# Atomic mobility in nanostructured liquid Ga–In alloy

E V Charnaya<sup>1,2</sup>, Cheng Tien<sup>1,3</sup>, M K Lee<sup>1</sup> and Yu A Kumzerov<sup>4</sup>

<sup>1</sup> Department of Physics, National Cheng Kung University, Tainan 70101, Taiwan, Republic of China

<sup>2</sup> Institute of Physics, St Petersburg State University, St Petersburg, Petrodvorets, 198504, Russia

<sup>3</sup> Center for Micro/Nano Science and Technology, National Cheng Kung University, Tainan 70101, Taiwan, Republic of China

<sup>4</sup> A F Ioffe Physico-Technical Institute RAS, St Petersburg, 194021, Russia

Received 5 January 2010, in final form 22 March 2010

Published 23 April 2010

Online at [stacks.iop.org/JPhysCM/22/195108](http://stacks.iop.org/JPhysCM/22/195108)

## Abstract

Nuclear spin relaxation and the Knight shift for  $^{71}\text{Ga}$ ,  $^{69}\text{Ga}$ , and  $^{115}\text{In}$  isotopes were studied by nuclear magnetic resonance (NMR) in liquid gallium–indium alloy confined to porous glass and alloy surface film and were compared with the bulk counterparts. Drastic spin relaxation acceleration under nanoconfinement was observed for the three isotopes. Quadrupole and magnetic contributions to spin relaxation were separated for gallium and indium isotopes using the experimental data obtained, which allowed, in particular, the evaluation of correlation times of atomic mobility. The strong decrease in the correlation time was found for confined alloy which evidenced a remarkable diffusion slowdown. The effect of changes in atomic mobility on NMR line broadening was also discussed.

## 1. Introduction

A great deal of attention has focused recently on the influence of confined geometry on atomic and molecular mobility in liquids. Studies of dynamics in confined liquids were primarily stimulated by strong interest in flowing through various porous media such as rocks, concretes, sands, and biological tissues. Self-diffusion alterations in liquids within pores can also affect catalytic processes, filtration rate, lubrication, melting and freezing phase transitions, and some aspects of the fabrication of nanostructures. From a fundamental viewpoint, studies of diffusion in liquids under nanoconfinement are of importance for better understanding general properties of low-dimensional systems. Translational and rotational diffusion was observed in a variety of liquids embedded into different nanoporous matrices such as zeolites, porous glasses, photonic crystals, and coals (see [1–4] and references therein). Changes of mobility in confined liquids compared to those in their bulk counterparts were shown to depend on pore sizes, liquid structure, interaction with the inner pore surface, geometry, and connectivity of the pore network.

Lately, NMR has been applied to some liquid metals introduced into porous glasses and opal photonic crystals (see [5–9] and references therein). Information on self-diffusion in the melted gallium and indium metals was obtained

through measurements of the nuclear spin relaxation rate. The observed drastic acceleration of the quadrupole contribution to spin relaxation evidenced a remarkable slowdown of mobility under nanoconfinement which became more pronounced with decreasing pore sizes. Until now, pure gallium and indium have remained the only two metals for which the effect of confinement on mobility in liquid state has been studied. For gallium, the occurrence of two isotopes,  $^{71}\text{Ga}$  and  $^{69}\text{Ga}$ , with quite distinctive quadrupole moments and gyromagnetic ratios facilitated the separation of quadrupole spin relaxation and quantitative treatment of experimental data contrary to the case of indium, the isotopes of which  $^{115}\text{In}$  and  $^{113}\text{In}$  have similar NMR properties, thus making useless any comparison of data for them and leaving some uncertainty about the quadrupole relaxation rate in confined geometry as well as in bulk.

In the present paper we report results of NMR studies of a Ga–In melted alloy confined to a porous glass with pore diameter 5 nm, thin liquid film of the same composition on the porous glass specimen surface and the bulk counterpart. It will be shown that the NMR measurements on three isotopes,  $^{71}\text{Ga}$ ,  $^{69}\text{Ga}$ , and  $^{115}\text{In}$ , allow us to develop a self-consistent treatment of spin relaxation, evaluate the correlation time of atomic mobility which will be found to decrease drastically for the confined Ga–In melt and estimate unambiguously

**Table 1.** The Knight shift ( $K$ ), linewidth at half height ( $\Delta$ ), total longitudinal relaxation time ( $T_1$ ), and times corresponding to magnetic ( $T_{1m}$ ) and quadrupole ( $T_{1q}$ ) contributions to longitudinal spin relaxation for the Ga–In alloy. Values of the Knight shift for  $^{69}\text{Ga}$  are the same as for  $^{71}\text{Ga}$ .

Isotope Alloy	$^{71}\text{Ga}$			$^{69}\text{Ga}$			$^{115}\text{In}$		
	Bulk	Surface	Confined	Bulk	Surface	Confined	Bulk	Surface	Confined
$K$ (ppm)	$4256 \pm 1$	$4253 \pm 1$	$4040 \pm 10$				$8502 \pm 2$	$8495 \pm 3$	$8300 \pm 20$
$\Delta$ (ppm)	$6.0 \pm 0.5$	$10 \pm 1$	$130 \pm 10$	$6.5 \pm 0.5$	$11 \pm 1$	$230 \pm 15$	$18 \pm 1$	$30 \pm 2$	$250 \pm 20$
$T_1$ ( $\mu\text{s}$ )	$522 \pm 3$	$500 \pm 10$	$54 \pm 3$	$649 \pm 5$	$580 \pm 30$	$23 \pm 4$	$222 \pm 8$	$183 \pm 15$	$7.5 \pm 1.5$
$T_{1m}$ ( $\mu\text{s}$ )	$577 \pm 9$			$931 \pm 15$			$410 \pm 40$		
$T_{1q}$ ( $\mu\text{s}$ )	$5500 \pm 800$	$3700 \pm 600$	$60 \pm 4$	$2100 \pm 400$	$1500 \pm 300$	$24 \pm 4$	$480 \pm 40$	$329 \pm 50$	$7.6 \pm 1.5$

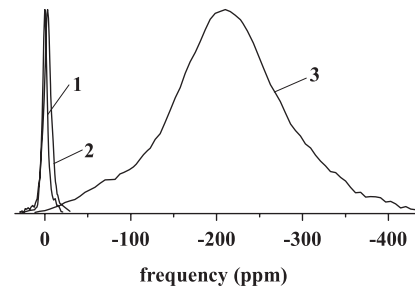
the quadrupole and magnetic contributions to spin relaxation for indium. The results obtained will extend the list of known metallic melts which manifest strong atomic mobility slowdown with decreasing dimensions.

## 2. Sample and experiment

The porous glass used in the present work as a matrix was made from a phase-separated soda borosilicate glass with pore structure produced by acid leaching. The mean pore size 5 nm was determined using mercury intrusion porosimetry which also showed that 80% of the pore volume corresponded to the size range from 4.8 to 5.4 nm. The liquid gallium–indium alloy of composition 90 at.% of Ga and 10 at.% of In was embedded into pores under high pressure up to 9 kbar. After filling the pores, the sample surface was thoroughly cleaned. The filling factor of the pore volume evaluated by weighing the sample was about 70%. After the sample was kept for several days, a discontinuous thin film was formed on the sample surface by a small amount of the alloy flowing out from pores. The thickness of the film on the surface was determined by optical microscopy as about 3–5  $\mu\text{m}$ . The total amount of the alloy estimated to be on the sample surface was small and did not affect noticeably the pore filling. Bulk Ga–In alloy of the same composition was also studied to make a comparison.

The liquidus temperature of bulk Ga–In alloy of the composition under study is near 20 °C [10], so it is liquid at room temperature (295 K) in agreement with our observations. The alloy on the surface and within pores is also completely melted at room temperature. Therefore, studies of mobility in bulk, surface, and confined alloy were carried out at 295 K.

Nuclear spin–lattice relaxation, lineshape, and the Knight shift for both gallium isotopes,  $^{71}\text{Ga}$  and  $^{69}\text{Ga}$ , and for  $^{115}\text{In}$  in the melted gallium–indium alloy were measured at a magnetic field of 9.4 T using a Bruker Avance 400 pulse spectrometer. The operating frequencies were about 122.4, 96.5, and 88.5 MHz, respectively. The inversion recovery procedure was applied to observe longitudinal spin relaxation. Magnetization recovery was monitored several times and the mean relaxation times were evaluated. The error of the calculated mean values was mainly due to the distribution of individual measurements and was characterized by the standard deviation of the mean. To detect the NMR line, a single pulse sequence with phase cycling was used. The repetition time was 0.15 s. Since the signals were rather faint, the number of scans varied from 2 to 8000. The Knight shift for the gallium isotopes was measured as the position of NMR line

**Figure 1.**  $^{71}\text{Ga}$  NMR line for Ga–In alloy: 1—bulk, 2—surface, 3—confined. Frequency is referenced to the signal from bulk.

peaks relative to the NMR signal from a GaAs single crystal. For  $^{115}\text{In}$  the line position in a 1 mol water solution of indium sulfate was used as a reference.

The two gallium isotopes have slightly different abundance, spin equal to 3/2, and distinct gyromagnetic ratios  $\gamma$  and quadrupole moments  $Q$  ( $\gamma(^{71}) = 8.18 \times 10^7 \text{ rad T}^{-1} \text{ s}^{-1}$ ,  $Q(^{71}) = 0.107 \text{ barn}$  and  $\gamma(^{69}) = 6.44 \times 10^7 \text{ rad T}^{-1} \text{ s}^{-1}$ ,  $Q(^{69}) = 0.171 \text{ barn}$  for  $^{71}\text{Ga}$  and  $^{69}\text{Ga}$ , respectively). The spin, gyromagnetic ratio and quadrupole moment of the  $^{115}\text{In}$  isotope are  $I = 9/2$ ,  $\gamma(\text{In}) = 5.90 \times 10^7 \text{ rad T}^{-1} \text{ s}^{-1}$  and  $Q(\text{In}) = 0.81 \text{ barn}$ , respectively.

## 3. Experimental results

For the three isotopes,  $^{71}\text{Ga}$ ,  $^{69}\text{Ga}$ , and  $^{115}\text{In}$ , NMR spectra for bulk, confined, and surface liquid alloy consisted of single lines. The values of the Knight shift and linewidth at half height are collected in table 1. For the bulk Ga–In alloy the lines were relatively narrow, while for the confined alloy the lines were strongly broadened. The lines corresponding to the surface films were somewhat broader than in bulk, but noticeably narrower than under confinement. The lines for  $^{71}\text{Ga}$  and  $^{115}\text{In}$  are shown in figures 1 and 2 as an example. The Knight shift for gallium in bulk alloy relative to the position of the GaAs signal is by 22 ppm lower than in bulk liquid gallium at room temperature [11]. The Knight shift for indium in bulk alloy relative to the indium sulfate solution signal is by about 550 ppm higher than the value of the Knight shift in bulk liquid indium near its melting point [7]. For the thin film on the sample surface the lines are slightly shifted to low frequencies compared to those in bulk alloy, as can be seen from figures 1 and 2 and table 1. For gallium and indium isotopes in confined alloy, the Knight shifts are reduced by about 200 ppm compared to those in bulk.

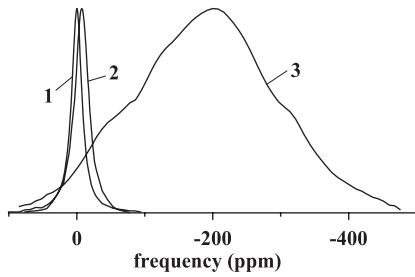


**Figure 2.**  $^{115}\text{In}$  NMR line for Ga–In alloy: 1—bulk, 2—surface, 3—confined. Frequency is referenced to the signal from bulk.

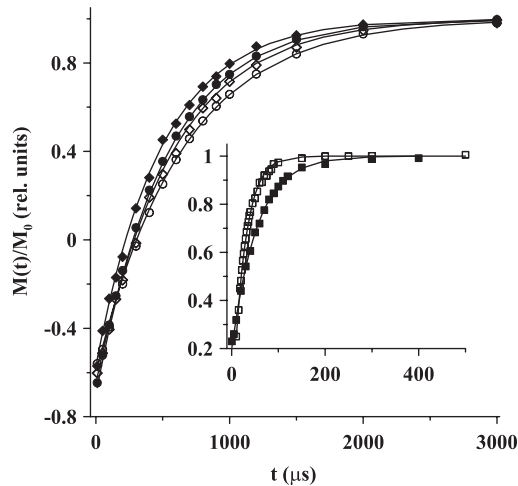


**Figure 3.** Magnetization recovery after a  $180^\circ$  pulse for bulk (circles), surface (diamonds), and confined (inset, squares) alloy. Closed and open symbols correspond to  $^{71}\text{Ga}$  and  $^{69}\text{Ga}$ , respectively. Solid lines are theoretical calculations as described in the text.

The recovery of the longitudinal nuclear magnetization for gallium and indium isotopes in bulk Ga–In alloy is single exponential as in other bulk liquid metals and alloys (figures 3 and 4). Single exponential relaxation is a result of fast self-diffusion in metallic melts leading to the extreme narrowing limit [12, 13]. The spin–lattice relaxation times for bulk alloy are listed in table 1. The values for  $^{71}\text{Ga}$  and  $^{69}\text{Ga}$  are slightly shorter than those obtained for bulk supercooled gallium at room temperature [6, 9, 13]. For instance, the relaxation times for bulk gallium in [6] were found to be 534 and 678  $\mu\text{s}$  for  $^{71}\text{Ga}$  and  $^{69}\text{Ga}$ , respectively. The  $^{115}\text{In}$  relaxation time in bulk alloy is a little bit longer than the relaxation time (188  $\mu\text{s}$ ) in pure liquid indium just near its melting point [5, 7].

For the liquid gallium thin film on the sample surface, longitudinal relaxation for both gallium isotopes is slightly accelerated while spin–lattice relaxation for the Ga–In alloy confined to nanopores is much faster than that in bulk and surface alloy. The experimental magnetization recovery curves for  $^{71}\text{Ga}$  and  $^{69}\text{Ga}$  in surface and confined alloy are shown in figure 3 along with the relaxation curves for bulk. Note that generally the extreme narrowing limit can be no longer valid for spin relaxation in confined alloy because of strong slowdown of atomic mobility, as will be discussed in section 4. In that case the magnetization recovery for spin 3/2 is

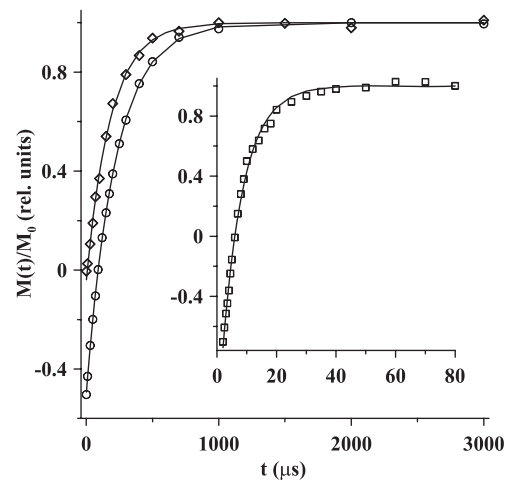


**Figure 4.**  $^{115}\text{In}$  magnetization recovery after a  $180^\circ$  pulse for bulk (circles), surface (diamonds), and confined (inset, squares) alloy. Solid lines are single exponential fits as described in the text.

described by a sum of two exponentials [14]. However, it was shown in [15] that the recovery curve remains quite similar to a single exponential and one can consider approximately the relevant times of recovery, which facilitates the comparison with relaxation in other samples. The times calculated under such an assumption are listed in table 1. As can be seen in table 1 and figure 3, relaxation in bulk and surface alloys is faster for the  $^{71}\text{Ga}$  isotope with higher gyromagnetic ratio while relaxation in confined alloy is faster for the  $^{69}\text{Ga}$  isotope with larger quadrupole moment.

The longitudinal magnetization recovery curves for  $^{115}\text{In}$  in surface and confined alloy are shown in figure 4 and the relevant recovery times are listed in table 1. As for gallium nuclei, relaxation becomes slightly faster in the alloy discontinuous film on the porous glass surface and is strongly accelerated under nanoconfinement.

#### 4. Discussion

Studies of nuclear spin relaxation in many liquid metals have shown that it occurs via coupling of nuclear magnetic moments with conduction electrons and of nuclear quadrupole moments with dynamic gradients of electric fields produced by atomic motion (see [13, 16] and references therein). The magnetic contribution is dominant in bulk melts where atomic mobility is fast and, therefore, the spectral density of electric field correlation function at the Larmor frequency is reduced. Because of fast atomic mobility and a short correlation time for conduction electrons, the extreme narrowing limit is valid for both contributions to spin relaxation and total relaxation is described by a single exponential with a relaxation time. The magnetic and quadrupole contributions to relaxation were clearly separated for metals which have more than one isotope since the quadrupole and magnetic relaxation rates are proportional to the squared nuclear quadrupole moment  $Q$  and gyromagnetic ratio  $\gamma$ , respectively [14]. In liquid metallic alloys the quadrupole contribution was found to increase compared to pure melts ([17, 18] and references therein). It

was suggested that the quadrupole relaxation acceleration in alloys was caused by rearrangement of atoms which led to the increase of electric gradients at nuclear sites [18]. When metals have only one isotope or when the NMR properties of isotopes are quite similar (as for In) the direct experimental separation of the magnetic and quadrupole contributions cannot be done. In those cases the rate of quadrupole and magnetic relaxation was estimated using theoretical predictions and experimental data on temperature dependences of relaxation. Such a procedure leaves an uncertainty concerning the comparative role of magnetic and quadrupole relaxation, which manifests itself in a large distribution of the quadrupole contribution magnitudes available in the literature, in particular, for indium [13, 19, 20]. Measurements on binary alloys do not remove completely such uncertainty. However, as it will be shown below, combining data for the three isotopes in bulk and surface Ga–In alloy allows us to evaluate the correlation time of atomic mobility for surface alloy and estimate accurately the quadrupole contribution to relaxation for indium. It also provides necessary information for calculations of the gallium and indium quadrupole relaxation rates and correlation time of atomic mobility under nanoconfinement using measurements of spin relaxation in confined alloy.

Let us first consider the results for the gallium isotopes. The total relaxation time for  $^{71}\text{Ga}$  in bulk alloy can be written as [13, 21]

$$T_{\text{lb}}^{-1}(71) = T_{\text{lqb}}^{-1}(71) + T_{\text{lmb}}^{-1}(71), \quad (1)$$

where the subscripts q and m indicate quadrupole and magnetic contributions, respectively. A similar relationship is valid for the  $^{69}\text{Ga}$  total relaxation time, however, using the general relations [21]  $T_{\text{lqb}}(69) = T_{\text{lqb}}(71)Q^2(71)/Q^2(69)$  and  $T_{\text{lmb}}(69) = T_{\text{lmb}}(71)\gamma^2(71)/\gamma^2(69)$  it can be rewritten as

$$T_{\text{lb}}^{-1}(69) = T_{\text{lqb}}^{-1}(71) \frac{Q^2(69)}{Q^2(71)} + T_{\text{lmb}}^{-1}(71) \frac{\gamma^2(69)}{\gamma^2(71)}. \quad (2)$$

The solution of these equations yields the relaxation times for magnetic and quadrupole contributions which are listed in table 1. These results can be compared with those obtained for bulk liquid pure gallium at room temperature in [6]. The magnetic contributions to relaxation of both isotopes proved to be quite similar in pure gallium and alloy, while the quadrupole contribution was enhanced in alloy. The enhancement of quadrupole coupling of the same order was also observed experimentally in Ga–In alloys of various compositions [17, 18]. Within the extreme narrowing limit, the quadrupole relaxation rate  $T_{\text{lqb}}^{-1}$  is proportional to the correlation time of atomic mobility in bulk alloy  $\tau_b$  [13, 19, 22]:

$$T_{\text{lqb}}^{-1}(71) = C_b(71)\tau_b \quad \text{and} \quad T_{\text{lqb}}^{-1}(69) = C_b(69)\tau_b, \quad (3)$$

where  $C_b(69) = C_b(71)Q^2(69)/Q^2(71)$  as was mentioned above. The correlation time  $\tau_b$  can be estimated from the diffusion coefficient  $D$ :  $\tau_b = d^2/6D$ , where  $d$  is the average interatomic distance. Since the diffusion coefficient in a liquid Ga–In alloy of about the same composition as studied here was found to be very similar to that in bulk pure gallium [23] we

will assume the correlation time in the bulk alloy under study to be the same as in bulk liquid gallium at room temperature:  $\tau_b = 1.4 \times 10^{-11}$  s [6]. This value agrees with earlier estimates for different liquid metals [13]. Then, one can find for the bulk Ga–In alloy from (3)  $C_b(71) = 1.3 \times 10^{13} \text{ s}^{-2}$  and  $C_b(69) = 3.3 \times 10^{13} \text{ s}^{-2}$ . They are slightly larger than for bulk liquid gallium [6], as expected.

For the alloy thin film on the porous glass surface the spin–lattice relaxation times for both gallium isotopes are reduced compared to bulk (see table 1 and figure 3). The acceleration of spin relaxation was also observed recently for gallium small isolated particles and for gallium and indium thin films on the surface of some porous matrices [6, 7, 24]. The relaxation enhancement in surface Ga–In alloy cannot be caused by an increase of the magnetic contribution. Actually, the relaxation time  $T_{\text{lm}}$  corresponding to the magnetic contribution to the total relaxation process is related to the Knight shift  $K$  by the general Korringa relation [25]:  $T_{\text{lm}}TK^2 = \text{const}/(\gamma\alpha)$ , where  $T$  is the temperature, and  $\alpha$  is the correction factor which accounts for the effects of electron correlation and exchange. Our measurements have shown that the Knight shift in liquid alloy on the surface was almost not changed compared to that in bulk alloy (table 1 and figure 1). Thus, the time  $T_{\text{lms}}$  for the alloy on the surface can be assumed to keep its bulk value  $T_{\text{lmb}}$  for both gallium isotopes.

The quadrupole relaxation time for  $^{71}\text{Ga}$   $T_{\text{lqs}}(71)$  can be evaluated by subtracting the magnetic contribution from the total relaxation rate using a relationship similar to (1) and the quadrupole relaxation time for  $^{69}\text{Ga}$  can be found as  $T_{\text{lqs}}(69) = T_{\text{lqs}}(71)Q^2(71)/Q^2(69)$ . The obtained values are listed in table 1. On the other hand,  $T_{\text{lqs}}(69)$  should satisfy a relation similar to (1) which leads to  $T_{\text{lqs}}(69) = 1540 \mu\text{s}$ . The difference between the two estimates for  $T_{\text{lqs}}(69)$  is within the accuracy of experiment and calculations. This confirms the self-consistency of the model developed. The single exponential fits corresponding to the model for  $^{71}\text{Ga}$  and  $^{69}\text{Ga}$  in bulk and surface alloy are shown in figure 3.

The increase in the quadrupole contribution to spin relaxation of gallium nuclei for the surface alloy can be caused by alterations in the correlation time  $\tau_s$  of atomic mobility or in the parameter of quadrupole coupling  $C$ . The spectral density of the correlation function of atomic motion in the low-frequency limit which determines the value of  $C$  for both gallium isotopes depends on the structure of melts [26, 27]. It is generally accepted that the structure of liquids does not change compared to bulk till size reduction below several nanometers [2, 28]. Therefore,  $C_s(71)$  and  $C_s(69)$  for the thin alloy film on the glass surface should keep their bulk values and the quadrupole relaxation acceleration occurs due to an increase in the correlation time  $\tau_s$ . Such an increase can be found from the following relationship  $\tau_s = \tau_b T_{\text{lqb}}(71)/T_{\text{lqs}}(71)$  which yields  $\tau_s = 2.0 \times 10^{-11}$  s and  $\tau_s/\tau_b = 1.4$ . Note that the latter ratio does not depend on the assumed value of  $\tau_b$ . Since the change in the correlation time is not strong, the extreme narrowing limit is still valid for spin relaxation in the surface alloy film.

Alterations in atomic mobility were also studied by NMR in a pure indium thin film of about the same thickness in [7].

The ratio between the correlation times in surface and bulk indium was found to be quite similar to that obtained above for Ga–In alloy:  $\tau_s/\tau_b = 1.6$ . A slowdown of mobility in a pure gallium thin film observed by neutron scattering was recently reported in [29].

Let us discuss now spin relaxation for indium. For  $^{115}\text{In}$  relaxation in bulk and surface alloy, two equations similar to relationship (1) can be written. Taking into account that the magnetic relaxation contributions are the same in bulk and surface because of very small alterations in the Knight shift and the quadrupole relaxation rates are given by  $T_{1qb}^{-1}(\text{In}) = C_b(\text{In})\tau_b$  and  $T_{1qs}^{-1}(\text{In}) = C_b(\text{In})\tau_s$ , the equations can be transformed to

$$\begin{aligned} T_{1b}^{-1}(\text{In}) &= C_b(\text{In})\tau_b + T_{1mb}^{-1}(\text{In}), \\ T_{1s}^{-1}(\text{In}) &= C_b(\text{In})\tau_s + T_{1mb}^{-1}(\text{In}). \end{aligned} \quad (4)$$

They include only two unknown values,  $C_b(\text{In})$  and  $T_{1mb}(\text{In})$ . The evaluated relaxation time  $T_{1mb}(\text{In})$  is given in table 1 along with other relaxation times for indium in bulk and surface alloy and  $C_b(\text{In})$  is equal to  $1.49 \times 10^{-10} \text{ s}^{-2}$ . The obtained quadrupole relaxation rate in bulk alloy ( $T_{1qb}^{-1}(\text{In}) = C_b(\text{In})\tau_b = 2080 \text{ s}^{-1}$ ) is just between two theoretical estimates reported for liquid indium near the melting point:  $3200 \text{ s}^{-1}$  [19] and  $1900 \text{ s}^{-1}$  [20]. Since many experimental studies confirmed the weak temperature dependence of the quadrupole relaxation rate (see [13, 18] and references therein) and since the total relaxation rate for  $^{115}\text{In}$  in the Ga–In alloys of similar composition was found to be about the same as the total relaxation rate in pure liquid indium [18], the evaluated  $T_{1qb}^{-1}(\text{In})$  can provide a good experimental estimate of the quadrupole contribution not only for the alloy, but for pure indium near its melting point as well. The found value of  $T_{1qb}^{-1}(\text{In})$  virtually coincides with the rate of quadrupole relaxation ( $\sim 2100 \text{ s}^{-1}$ ) calculated in [30] for pure melted indium using temperature dependences of spin relaxation in liquid alloys.

The drastic acceleration of nuclear spin relaxation for  $^{71}\text{Ga}$ ,  $^{69}\text{Ga}$ , and  $^{115}\text{In}$  under nanoconfinement shown in figures 3 and 4 cannot be caused by alterations in the magnetic contribution either since the Knight shift was decreased by less than 5%, which according to the Korringa relation could lead only to some slight relaxation rate reduction. Therefore, as in the case of pure liquid gallium and indium [5–9] we should assume that nanoconfinement affected remarkably the quadrupole contribution to spin relaxation. In agreement with such a suggestion, spin relaxation for the  $^{69}\text{Ga}$  isotope with larger quadrupole moment was faster in confined alloy than for  $^{71}\text{Ga}$  (figure 3) which means that quadrupole relaxation becomes dominant for the alloy within pores.

To model the quadrupole relaxation acceleration for gallium isotopes under nanoconfinement we will use the general relationship developed in [14] for quadrupole relaxation of nuclei with spin 3/2:

$$\begin{aligned} \frac{M(t)}{M_0} &= 1 - b \left[ \frac{4}{5} \exp\left(-2\left(\frac{eQ}{\hbar}\right)^2 J_{-22}(2\omega_0)t\right) \right. \\ &\quad \left. + \frac{1}{5} \exp\left(2\left(\frac{eQ}{\hbar}\right)^2 J_{-11}(\omega_0)t\right) \right], \end{aligned} \quad (5)$$

where  $M(t)$  and  $M_0$  are time-dependent and equilibrium magnetizations, respectively,  $1 - b$  is the starting relative magnetization,  $e$  is the electron charge,  $\omega_0$  is the Larmor frequency,  $J_{-ii}(\omega)$  are the spectral densities of the electric field gradient correlation function at the nuclear site. Assuming that the correlation function of atomic mobility is represented by  $\exp(-t/\tau_c)$  [12], where the subscript c refers to confined geometry, and taking into account the magnetic contribution, one can get the following relationship for total relaxation of  $^{71}\text{Ga}$  nuclei

$$\begin{aligned} \frac{M(t)}{M_0} &= 1 - b \left[ \frac{4}{5} \exp\left(-\frac{C_c(71)\tau_c t}{1 + 4\omega_{71}^2\tau_c^2}\right) \right. \\ &\quad \left. + \frac{1}{5} \exp\left(-\frac{C_c(71)\tau_c t}{1 + \omega_{71}^2\tau_c^2}\right) \right] \exp\left(-\frac{t}{T_{1mb}(71)}\right). \end{aligned} \quad (6)$$

In (6)  $\omega_{71}$  is the Larmor frequency for  $^{71}\text{Ga}$ . A similar relationship can be written for  $^{69}\text{Ga}$ . In (6) the time of magnetic relaxation was assumed to be the same as in bulk. Actually, since the Knight shift under nanoconfinement was reduced (table 1 and figures 1 and 2), one can expect according to the Korringa relation a relevant increase in the magnetic relaxation time by about 10%. However, under nanoconfinement, magnetic relaxation is much slower than in the quadrupole case (see table 1) and the small alteration in the magnetic relaxation time does not influence noticeably the estimate for the rate of quadrupole relaxation.

Equation (6) predicts that the quadrupole relaxation is fastest when  $\omega_{71}\tau_c \cong 0.5$  and becomes less effective at decreasing and increasing  $\tau_c$ . If we assume that the values  $C_c(71)$  and  $C_c(69)$  do not change compared to those in the bulk and surface, relaxation according to (6) and a similar relationship for  $^{69}\text{Ga}$  will be much slower than the experimentally observed relaxation at any values of  $\tau_c$ . The minimal possible  $C_c(71)$  which ensures fast enough relaxation for  $^{71}\text{Ga}$  is equal to  $4.7 \times 10^{13} \text{ s}^{-2}$  which is noticeably higher than the relevant value in bulk alloy. However, the best fitting for both gallium isotopes was obtained by setting  $C_c(71) = 7 \times 10^{13} \text{ s}^{-2}$  and  $\tau_c = 2.7 \times 10^{-10} \text{ s}$ ,  $C_c(69)$  being calculated using the relationship  $C_c(69) = C_c(71)Q^2(69)/Q^2(71) = 1.8 \times 10^{14} \text{ s}^{-2}$ . The ratio  $\tau_c/\tau_b = 19$  evidences a remarkable slowdown of atomic mobility under nanoconfinement. The fit is shown in figure 3. The extreme narrowing limit for such a long correlation time is no longer quite justified for  $^{71}\text{Ga}$  which has the highest Larmor frequency, but still is plausible for  $^{69}\text{Ga}$  and  $^{115}\text{In}$ . Nevertheless, since the difference between an accurate dependence given by (6) and single exponential recovery with an appropriate relaxation time is not very pronounced [15], the effective quadrupole relaxation time  $T_{1qc}(71)$  for  $^{71}\text{Ga}$  within nanopores can also be evaluated. The quadrupole relaxation times calculated for two gallium isotopes are given in table 1. Note that the increase in the electric field gradients at the nucleus sites which determine the magnitude of  $C$  was also obtained for liquid pure gallium embedded into porous glasses with pore sizes less than 8 nm [6].

Relaxation for indium nuclei in confined alloy under the assumption of the extreme narrowing limit obeys the relationship

$$T_{1c}^{-1}(\text{In}) = C_c(\text{In})\tau_c + T_{1mb}^{-1}(\text{In}), \quad (7)$$

where the total relaxation time  $T_{1c}(\text{In})$  is given in table 1. Relationship (7) yields the estimate  $C_c(\text{In}) = 4.8 \times 10^{14} \text{ s}^{-2}$ . It is also higher than in bulk alloy. The single exponential fit for the  $^{115}\text{In}$  magnetization recovery under confinement is shown in figure 4 and the calculated time of quadrupole relaxation  $T_{1qc}(\text{In})$  is included into table 1. One can see that quadrupole relaxation became dominant for  $^{115}\text{In}$  in the melted Ga–In alloy within nanopores similarly to quadrupole relaxation for  $^{71}\text{Ga}$  and  $^{69}\text{Ga}$ .

As follows from the ratio  $\tau_c/\tau_b$  obtained above, nanoconfinement leads to an increase of the correlation time by a factor of about 20. Since the self-diffusion coefficient is inversely proportional to the correlation time, the results obtained show a remarkable slowdown of self-diffusion in Ga–In alloy caused by confined geometry. Note that the slowdown of self-diffusion is already quite noticeable for a surface film of several micrometers in thickness.

The increase in the correlation time of atomic mobility for alloy within nanopores and on the surface should also influence the quadrupole contribution to transverse spin relaxation for the gallium and indium isotopes. The quadrupole contribution to transverse magnetization recovery for spin 3/2 in liquids is given by the relationship [14]

$$\frac{M_{\perp}(t)}{M_0} = \frac{3}{5} \exp\left[-\frac{1}{2}C\tau t \left(\frac{1}{1+\omega_0^2\tau^2} + 1\right)\right] + \frac{2}{5} \exp\left[-\frac{1}{2}C\tau t \left(\frac{1}{1+\omega_0^2\tau^2} + \frac{1}{1+4\omega_0^2\tau^2}\right)\right], \quad (8)$$

where  $M_{\perp}(t)$  is the time-dependent transverse magnetization. Within the extreme narrowing approximation, relationship (8) when combined with magnetic relaxation in metals reduces to a single exponential decay with a relaxation time  $T_2 = T_1$ . The latter relation does not depend on the spin value. Assuming that the extreme narrowing limit is valid in all cases except  $^{71}\text{Ga}$  in confined alloy, one can calculate the transverse magnetization decay using the equality  $T_2 = T_1$  for all three isotopes in bulk and surface alloy and for  $^{69}\text{Ga}$  and  $^{115}\text{In}$  in confined alloy and relationship (8) for  $^{71}\text{Ga}$  in confined alloy and to estimate the NMR linewidths. Such estimates predict NMR line broadening for surface and confined alloy compared to bulk. The predicted trend corresponds to the experimentally observed broadening for the three isotopes. However, in confined alloy the NMR lines are somewhat broader than estimated, while their width is still dominated by dynamic broadening. This evidences the influence of some additional mechanism of broadening. Similar excess in NMR line widths was observed for pure liquid gallium and indium within nanopores [5, 7, 9] and probably is caused by inhomogeneous broadening due to different Knight shifts in pores of different sizes.

The decrease in the Knight shift caused by nanoconfinement (see table 1) was also observed for liquid gallium, indium, mercury, and tin metals embedded into nanoporous matrices [7, 11, 31, 32]. For pure melted gallium confined to porous glass with a 5 nm pore size, the decrease in the Knight shift compared to bulk at room temperature was 74 ppm [11] which is about one third of that obtained for Ga–In alloy (figure 1). The decrease in the Knight shift for pure indium was measured only in indium loaded porous glass with a 7 nm

pore size [7]. It was found to be near 100 ppm. Taking into account that the Knight shift was found in confined liquid metals [11, 31] to decrease linearly or weaker than linearly with increasing the inversed pore size, one can estimate the maximal decrease in the Knight shift for pure liquid indium within pores of 5 nm as 140 ppm. The decrease in the Knight shift for indium in confined Ga–In alloy is noticeably larger than this estimate. Then we can conclude that size effects on the Knight shift are more pronounced in Ga–In alloy than in pure liquid metals. Note that the changes in the Knight shifts in bulk Ga–In alloy compared to those in pure gallium and indium melts agree well with data obtained in [33].

In conclusion, NMR studies of spin–lattice relaxation for the  $^{71}\text{Ga}$ ,  $^{69}\text{Ga}$ , and  $^{115}\text{In}$  isotopes in liquid binary gallium–indium alloy embedded into a porous glass and in the alloy thin film on the porous glass surface revealed the enhancement of the relaxation rate for the three isotopes compared to bulk liquid alloy. The relaxation acceleration was very pronounced under nanoconfinement where the dominant mechanism of relaxation was changed from magnetic to quadrupolar. Experimental data obtained for two gallium isotopes,  $^{71}\text{Ga}$  and  $^{69}\text{Ga}$ , allowed the unambiguous separation of the magnetic and quadrupole contributions to total gallium spin relaxation in bulk, surface, and confined alloy and evaluation of the correlation time of atomic mobility for confined and surface alloy. For surface alloy the correlation time was found to be by a factor of 1.4 longer than in the bulk counterpart while under nanoconfinement the correlation time was about 20 times longer. The correlation times obtained were used to treat the experimental data for indium spin relaxation which allowed the direct separation of the quadrupole and magnetic contributions to relaxation of the  $^{115}\text{In}$  isotope in bulk as well as in surface and confined alloy. The evaluated quadrupole contribution to indium spin relaxation in bulk alloy provides a good approximation for the quadrupole relaxation in bulk pure indium which was previously only estimated theoretically and from temperature dependences of spin relaxation in indium alloys. The quadrupole relaxation enhancement in gallium–indium alloy under nanoconfinement and on the surface and the associated increase of the correlation times of atomic motion evidence the slowdown of atomic diffusion compared to bulk. The NMR line broadening for the three isotopes in surface and confined melted alloy was mainly related to the transverse relaxation acceleration which is also caused by the increase of the quadrupole contribution. However, for confined alloy an additional mechanism of line broadening is effective. The influence of confinement on the Knight shift of NMR lines was found to be stronger in Ga–In alloy than in pure gallium and indium metals.

## References

- [1] Kärger J and Ruthven D M 1992 *Diffusion in Zeolites and Other Microporous Solids* (New York: Wiley)
- [2] Drake J M, Klafter J, Levitz P E, Overney R M and Urbakh M (ed) 2001 *Dynamics in Small Confining Systems V* (Warrendale, PA: MRS)
- [3] Weber M, Klemm A and Kimmich R 2001 *Phys. Rev. Lett.* **86** 4302

- [4] Levitz P, Korb J P and Petit D 2003 *Eur. Phys. J. E* **12** 29
- [5] Charnaya E V, Tien Ch, Lee M K and Kumzerov Yu A 2007 *Phys. Rev. B* **75** 212202
- [6] Charnaya E V, Tien Ch, Wang W, Lee M K, Michel D, Yaskov D, Sun S Y and Kumzerov Yu A 2005 *Phys. Rev. B* **72** 035406
- [7] Charnaya E V, Tien Ch, Kumzerov Yu A and Fokin A V 2004 *Phys. Rev. B* **70** 052201
- [8] Lee M K, Charnaya E V and Tien Ch 2008 *Microelectron. J.* **39** 566
- [9] Charnaya E V, Loeser T, Michel D, Tien Ch, Yaskov D and Kumzerov Yu A 2002 *Phys. Rev. Lett.* **88** 097602
- [10] White C E T and Okamoto H 1992 *Phase Diagrams of Indium Alloys and their Engineering Applications, Monograph Series on Alloy Phase Diagrams* (Materials Park, OH: ASM International)
- [11] Charnaya E V, Michel D, Tien Ch, Kumzerov Yu A and Yaskov D 2003 *J. Phys.: Condens. Matter* **15** 5469
- [12] Abragam A 1989 *Principles of Nuclear Magnetism* (Oxford: Clarendon)
- [13] Titman J M 1977 *Phys. Rep.* **33** 1
- [14] Hubbard P S 1970 *J. Chem. Phys.* **53** 985
- [15] Tokuhito T 1988 *J. Magn. Reson.* **76** 22
- [16] Rossini F A and Knight W D 1969 *Phys. Rev.* **178** 641
- [17] Quitmann D 1990 *Hyperfine Interact.* **62** 237
- [18] Cartledge G, Havill R L and Titman J M 1976 *J. Phys. F: Met. Phys.* **6** 639
- [19] Sholl C A 1967 *Proc. Phys. Soc.* **91** 130
- [20] Rossini F A, Geissler E, Dickson E M and Knight W D 1967 *Adv. Phys.* **16** 287
- [21] Kerlin A L and Clark W G 1975 *Phys. Rev. B* **12** 3533
- [22] Sholl C A 1974 *J. Phys. F: Met. Phys.* **4** 1556
- [23] Dereball R and Koster J N 1998 *Int. J. Heat Mass Transfer* **41** 2537
- [24] Tien Ch, Charnaya E V, Sedykh P and Kumzerov Yu A 2003 *Phys. Solid State* **45** 2352
- [25] Carter G C, Bennett L H and Kahan D J 1977 *Metallic Shifts in NMR* (Oxford: Pergamon)
- [26] Bosse J, Quitmann D and Wetzel C 1983 *Phys. Rev. A* **28** 2459
- [27] Warren W W Jr 1974 *Phys. Rev. A* **10** 657
- [28] Christenson H K 2001 *J. Phys.: Condens. Matter* **13** R95
- [29] Konrad H, Weissmüller J, Birringer R, Karmonik C and Gleiter H 1998 *Phys. Rev. B* **58** 2142
- [30] Brandenburg R, Kokavec B and Kramer K 1977 *J. Phys. F: Met. Phys.* **7** 2593
- [31] Tien Ch, Charnaya E V, Lee M K and Kumzerov Yu A 2007 *J. Phys.: Condens. Matter* **19** 106217
- [32] Charnaya E V, Tien Ch, Lee M K and Kumzerov Yu A 2007 *Phys. Rev. B* **75** 144101
- [33] Moulson D J and Seymour E F W 1967 *Adv. Phys.* **16** 449